For 10% oxygen the displacement field has been calculated from (3) and (5) for a single defect and is shown in Fig. 5. This field, when linearly superimposed with $n-1$ similar fields gives the correct lattice expansion for 10% oxygen or n defects. The displacements are small, about 0·015 Å at the position of the nearest Ti atoms. In the vicinity of the interstitial oxygen they are obviously unrealistic considering the rapid variation of the displacement within the volume of the Ti atom. It may be concluded that the detailed features of the displacement field have no physical basis. Its merit lies in the fact that it gives the correct lattice expansion and the right order of magnitude for the LB intensity reduction. Other physically more satisfying models may do the same. However, by using a similar elastic model it is possible to estimate the defect concentration for other systems by measuring the lattice parameter and intensity changes. The Ti–O results show that the right order of magnitude for the concentration can be obtained in this manner.

The authors wish to thank Mr. W. Benner for his help in collecting X-ray data at FIL.

References

Anderson, O. L. (1963). *Phys. Chem. Solids,* **24**, 909.

Andersson, S., Collen, B., Kuylenstierna, U. & Magnéli, A. (1957). *Acta Chem. Scand.* **11**, 1641.

Annaka, S. (1962). *J. Phys. Soc. Japan,* **17**, 846.

Cochran, W. & Kartha, G. (1956). *Acta Cryst.* **9**, 944.

Ekstein, M. G. (1945). *Phys. Rev.* **68**, 120.

Eshelby, J. D. (1956). *Solid State Physics,* **3**, 79.

Fisher, K. & Hahn, H. (1963). *Z. Phys.* **172**, 172.

Flinn, P. A. & Maradudin, A. A. (1962). *Ann. Physics,* **18**, 81.

Freeman, A. J. (1959). *Acta Cryst.* **12**, 261.

Garland, C. W. & Slutzky, L. J. (1958). *J. Chem. Phys.* **28**, 331.

Huang, K. (1947). *Proc. Roy. Soc.* A, **190**, 102.

James, R. W. (1958). *The Optical Principles of the Diffraction of X-Rays,* p. 237. London: Bell.

Joel, N., Vera, R. & Garaychochea, I. (1953). *Acta Cryst.* **6**, 465.

Kanzaki, H. (1957). *Phys. Chem. Solids,* **2**, 24, 107.

Kaufman, L. (1961). ASD Technical Report 61-445.

Kothen, C. W. & Johnston, H. L. (1953). *J. Amer. Chem. Soc.* **75**, 3101.

Krivoglaz, M. A. (1959). *Fiz. Metal. Metalloved.* **7**, 650.

Kröner, E. (1953). *Z. Phys.* **136**, 402.

Kröner, E. (1958). *Kontinuumstheorie der Versetzungen und Eigenspannungen, Ergebnisse der Angewandten Mathematic.* Vol. 5. Berlin: Springer.

Leibfried, G. (1953). *Z. Phys.* **135**, 23.

Matsubara, T. (1952). *J. Phys. Soc. Japan,* **7**, 270.

Qurashi, M. M. (1954). *Acta Cryst.* **7**, 310.

Schoening, F. R. L. & Witt, F. (1963). *Advanc. X-Ray Analysis,* **6**, 136. (W. M. Mueller & M. Fay, Editors). New York: Plenum Press.

Teltow, J. (1953). *Ann. Phys. Lpz.* **12**, 111.

Wolcott, N. M. (1959). *J. Chem. Phys.* **31**, 536.

Zachariasen, W. H. (1945). *Theory of X-Ray Diffraction in Crystals.* New York: Wiley.

Zener, C. (1936). *Phys. Rev.* **49**, 122.

Acta Cryst. (1965). **18**, 614

The Crystal and Molecular Structure of $Fe(CO)_3(C_6H_5C_2C_6H_5)_2$

By R. P. Dodge and V. Schomaker

Union Carbide Research Institute, P. O. Box 278, Tarrytown, New York, U.S.A.

(*Received* 24 *April* 1964 *and in revised form* 25 *June* 1964)

A single-crystal X-ray diffraction study of $Fe(CO)_3(C_6H_5C_2C_6H_5)_2$ has shown it to be tetraphenylcyclobutadiene iron tricarbonyl. The final refined structure shows the cyclobutadiene ring to be square planar with ring-bond distance 1·46 Å.

Introduction

The yellow crystalline substance $Fe(CO)_3(C_6H_5C_2C_6H_5)_2$, one of a series of "tolane iron carbonyl complexes", was prepared and studied by Hübel, Braye, Clauss, Weiss, Krüerke, Brown, King & Hoogzand (1959). This product of the reaction of $Fe(CO)_5$ and diphenylacetylene was found to be stable at the melting point (234 °C) in contrast to other compounds in this series. Reductive degradation indicated that the two tolane molecules do not form separate ligands.

One of the anticipated structures was that of tetraphenylcyclobutadiene iron tricarbonyl and this possibility was confirmed by X-ray diffraction. The preliminary results were the subject of an earlier note (Dodge & Schomaker, 1960). The present paper is a presentation of the complete results from least-squares refinement.

Experimental

The crystal used, a flat square plate approximately 200 μ on a side and 60 μ thick, was selected from a sample suppled by Dr. Hübel.

A zirconium-filtered Mo $K\alpha$ source was used to collect a total of 2204 independent reflections, of which

1776 counted higher than background. The stationary-crystal, stationary-counter method was employed with a G.E. single crystal orienter. Each reflection was counted for 10 seconds. Background levels were estimated from a survey away from the Bragg peaks and the associated white radiation streaks. The stronger peaks are therefore better determined than those near the background level.

The crystals are monoclinic with $a = 8{\cdot}93$ Å, $b = 18{\cdot}72$ Å, $c = 14{\cdot}09$ Å, and $\beta = 92{\cdot}7°$, systematic absences corresponding to $P2_1/c$, and density 1·39 g.cm^{-3}. The density calculated for 4 molecules per unit cell

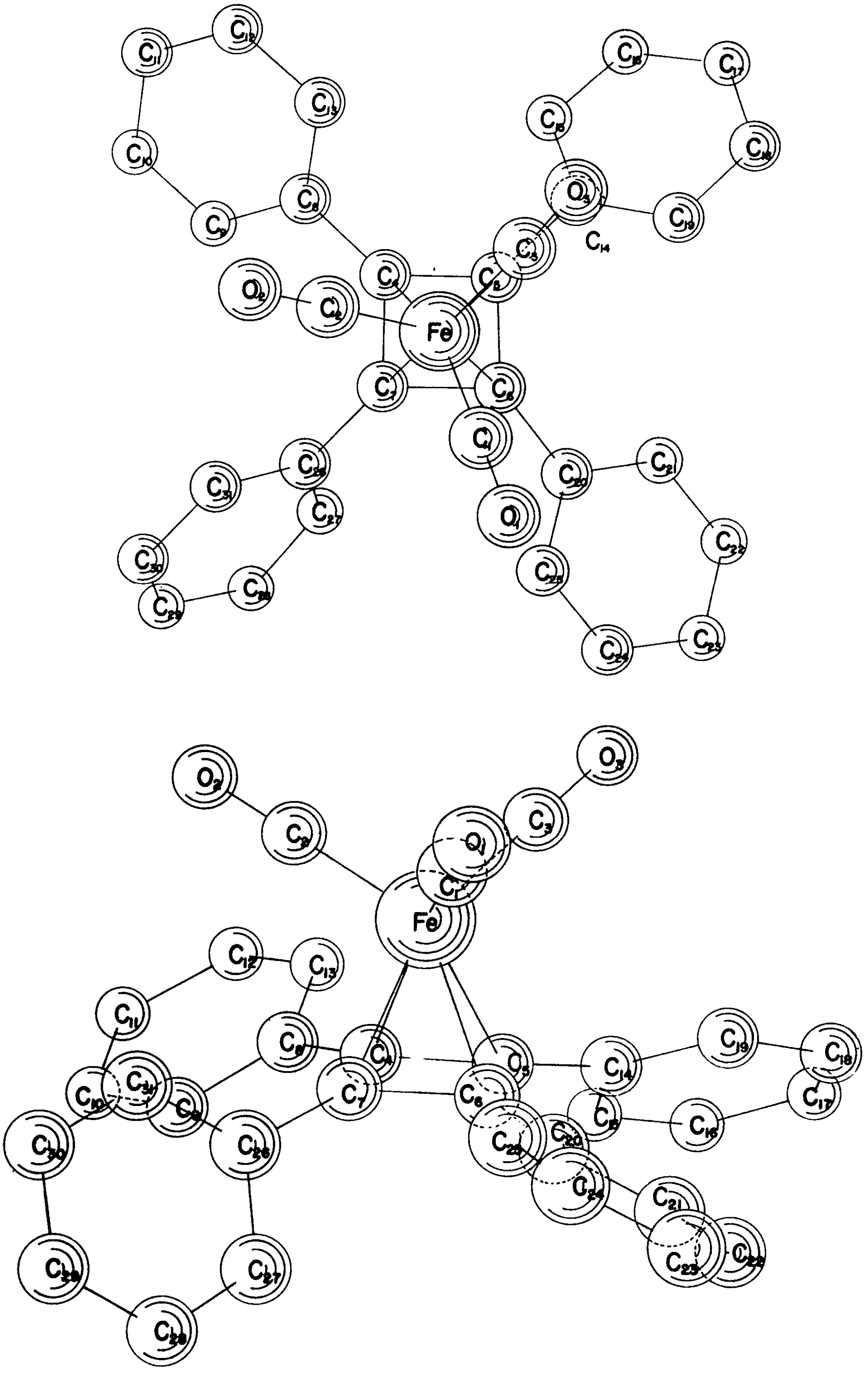

Fig. 1. Two views of the $Fe(CO)_3(C_6H_5C_2C_6H_5)_2$ molecule. In the lower diagram, which shows the molecule viewed along **b**, the traces of **a** and **c** are directed toward the right, respectively about 30° above and 60° below the horizontal.

is 1·40 g.cm^{-3}. The calculated linear absorption coefficient (μ) is about 7·0 cm^{-1}, so that variation of the absorption factor was negligible.

The three-dimensional Patterson function clearly showed the iron atom interactions. Three-dimensional superposition carried out graphically, with sections of the vector map, then led to the locations of all but two atoms in the complete molecule, even though only the arbitrary zero line of the Patterson function was used. An electron density Fourier then revealed the complete structure.

The program of Trueblood, Sparks & Gantzel, modified for use on the IBM 7094 computer at Union Carbide, was used for a full-matrix least-squares refinement of the structure. Individual isotropic temperature factors were used in the calculation. Unit weights for all reflections, except those with observed count less than estimated background, which were given zero weight, led to a final $R=\Sigma|\Delta F|/\Sigma F_o$, including all 2204 reflections, of 0·134.

Discussion

Fig. 1 gives two views of the molecule. One view (lower diagram) is along **b**; the other view is a general view looking down the line from the center of the cyclobutadiene ring to the iron atom. The cyclobutadiene ring is presumably stabilized by the bonding to iron, but even so, the thermal stability of the substance is perhaps surprising in view of the apparent instability of tetraphenylcyclobutadiene itself. Other iron carbonyl complexes with the butadiene residue show that when only one iron atom is present the bonding is invariably between it and the π bonding orbitals of the butadiene residue. When more than one iron atom is available per butadiene residue, one of the iron atoms forms a planar five-membered ring with the butadiene unit.

The final parameters values are given in Table 1. Some of the important bond distances and angles along with the corresponding estimated standard deviations are given in Table 2. The twenty-four bond distances in the phenyl rings average 1·406 Å in length with an average deviation of 0·022 Å.

The cyclobutadiene ring is square planar to well within the accuracy of the determination, the carbon–carbon bond distances averaging 1·459 Å. The cyclobutadiene ring also occurs with average bond length 1·431 Å and average deviation 0·024 Å in 1,2,3,4-tetramethylcyclobutadiene-nickel dichloride, (Dunitz, Mez, Mills & Shearer, 1962). Their results were affected by a disorder in the position of a solvated benzene molecule.

Table 1. *Final atomic parameters*

Atom	x	σ_x	y	σ_y	z	σ_z	B	σ_B
Fe	0·0899	0·0002	0·1949	0·0001	−0·0119	0·0001	2·73	0·05
O(1)	0·1796	0·0011	0·0468	0·0005	−0·0476	0·0007	4·70	0·22
O(2)	−0·0852	0·0012	0·2231	0·0006	−0·1880	0·0008	5·50	0·25
O(3)	0·3748	0·0012	0·2582	0·0005	−0·0643	0·0007	4·95	0·23
C(1)	0·1428	0·0014	0·1074	0·0007	−0·0360	0·0009	3·24	0·28
C(2)	−0·0135	0·0015	0·2116	0·0007	−0·1179	0·0009	3·31	0·28
C(3)	0·2610	0·0015	0·2329	0·0007	−0·0435	0·0010	3·49	0·29
C(4)	−0·0395	0·0013	0·2631	0·0006	0·0636	0·0008	2·50	0·25
C(5)	0·1027	0·0013	0·2517	0·0007	0·1160	0·0009	2·64	0·26
C(6)	0·0653	0·0014	0·1777	0·0007	0·1316	0·0009	2·89	0·27
C(7)	−0·0804	0·0013	0·1884	0·0006	0·0808	0·0008	2·32	0·24
C(8)	−0·1243	0·0013	0·3237	0·0006	0·0256	0·0009	2·73	0·27
C(9)	−0·2799	0·0015	0·3246	0·0007	0·0328	0·0010	3·71	0·30
C(10)	−0·3649	0·0016	0·3822	0·0007	−0·0057	0·0010	4·32	0·33
C(11)	−0·2945	0·0017	0·4430	0·0008	−0·0509	0·0011	4·54	0·34
C(12)	−0·1396	0·0017	0·4394	0·0008	−0·0559	0·0010	4·32	0·33
C(13)	−0·0515	0·0016	0·3820	0·0008	−0·0184	0·0010	3·92	0·31
C(14)	0·2217	0·0013	0·3001	0·0007	0·1562	0·0008	2·74	0·25
C(15)	0·1797	0·0016	0·3697	0·0008	0·1830	0·0010	3·97	0·31
C(16)	0·2886	0·0018	0·4134	0·0009	0·2275	0·0012	5·39	0·37
C(17)	0·4350	0·0017	0·3881	0·0008	0·2453	0·0011	4·88	0·35
C(18)	0·4764	0·0017	0·3212	0·0008	0·2210	0·0010	4·58	0·34
C(19)	0·3680	0·0015	0·2752	0·0007	0·1727	0·0010	3·64	0·30
C(20)	0·1181	0·0013	0·1181	0·0007	0·1912	0·0009	2·66	0·26
C(21)	0·2150	0·0015	0·1284	0·0007	0·2735	0·0010	3·45	0·29
C(22)	0·2618	0·0016	0·0713	0·0008	0·3284	0·0011	4·52	0·34
C(23)	0·2171	0·0016	0·0035	0·0008	0·3067	0·0010	4·35	0·34
C(24)	0·1182	0·0017	−0·0103	0·0008	0·2253	0·0011	4·78	0·35
C(25)	0·0699	0·0015	0·0497	0·0007	0·1693	0·0010	3·76	0·30
C(26)	−0·2234	0·0014	0·1496	0·0007	0·0834	0·0009	2·89	0·26
C(27)	−0·2694	0·0015	0·1331	0·0007	0·1743	0·0010	3·50	0·29
C(28)	−0·4066	0·0015	0·0947	0·0007	0·1841	0·0010	3·76	0·30
C(29)	−0·4979	0·0016	0·0794	0·0008	0·1029	0·0010	4·37	0·33
C(30)	−0·4522	0·0016	0·0961	0·0008	0·0136	0·0010	4·49	0·33
C(31)	−0·3134	0·0015	0·1323	0·0007	0·0040	0·0010	3·66	0·30

Table 2. *Interatomic distances and bond angles*

Bond	Distance	σ	Bonds	Angle	σ
Fe–C(1)	1·742 Å	0·013	C(1)–Fe–C(2)	98·0°	0·6
Fe–C(2)	1·747	0·013	C(1)–Fe–C(3)	94·8	0·6
Fe–C(3)	1·762	0·014	C(2)–Fe–C(3)	98·1	0·6
Fe–C(4)	2·054	0·012	C(4)–Fe–C(5)	41·1	0·5
Fe–C(5)	2·091	0·012	C(4)–Fe–C(7)	41·9	0·5
Fe–C(6)	2·069	0·013	C(5)–Fe–C(6)	40·6	0·5
Fe–C(7)	2·055	0·012	C(6)–Fe–C(7)	41·7	0·5
C(1)–O(1)	1·195	0·016	O(1)–C(1)–Fe	176·6	1·2
C(2)–O(2)	1·171	0·017	O(2)–C(2)–Fe	178·7	1·2
C(3)–O(3)	1·172	0·017	O(3)–C(3)–Fe	179·8	1·2
C(4)–C(5)	1·454	0·017	C(5)–C(4)–C(7)	89·7	0·9
C(4)–C(7)	1·468	0·017	C(4)–C(5)–C(6)	90·9	1·0
C(5)–C(6)	1·445	0·017	C(5)–C(6)–C(7)	90·0	1·0
C(6)–C(7)	1·469	0·017	C(4)–C(7)–C(6)	89·4	0·9
C(4)–C(8)	1·452	0·017	C(5)–C(4)–C(8)	136·9	1·1
C(5)–C(14)	1·488	0·017	C(7)–C(4)–C(8)	132·4	1·1
C(6)–C(20)	1·461	0·017	C(4)–C(5)–C(14)	134·0	1·1
C(7)–C(26)	1·471	0·017	C(6)–C(5)–C(14)	133·8	1·1
			C(5)–C(6)–C(20)	138·5	1·1
			C(7)–C(6)–C(20)	129·7	1·1
			C(4)–C(7)–C(26)	134·2	1·1
			C(6)–C(7)–C(26)	132·1	1·1

In orientation relative to the four-membered ring the $Fe(CO)_3$ group is similar to the nickel chloride group in Dunitz's compound.

The substituent phenyl groups are bent out of the plane of the cyclobutadiene ring away from the iron atom an average of 10·8°. In addition, the phenyl groups in each molecule are all twisted in the same sense. Table 3 gives the angles of twist and bend for the phenyl groups designated by the adjacent carbon atom of the C_4 butadiene ring. It is apparent that the phenyl at C(7) is unusual. Although it is not as close as the other phenyl groups to a carbonyl group, no consistent intramolecular explanation is apparent for its special twist and bend, which rather seem to correspond to special features in the packing. In particular, atom C(30) is cradled by a pair of oxygen atoms from an adjacent molecule, and this seems to account for the observed asymmetry in the angle of bending and twisting of this phenyl group.

Table 3. *Angles of bend and twist for the phenyl groups*

Phenyl group	Angle of bend	Angle of twist
at C(4)	6·9°	32·4°
at C(5)	9·6	36·4
at C(6)	10·1	28·6
at C(7)	16·7	60·8

Errors and accuracy

As previously mentioned, the stronger reflections are well determined compared to the class of weak intensities. This is readily seen in Table 4, which shows how the R value changes with the magnitude of F_o. The table of F_o's was sorted in descending order of the F_o values and R was calculated for each group.

Table 4. *Change of R with magnitude of F_o*

Number of reflections	R for this group	Over-all R value
200 largest	0·046	0·046
400 largest	0·054	0·049
600 largest	0·078	0·056
800 largest	0·083	0·060
1000 largest	0·079	0·064
1200 largest	0·122	0·069
1400 largest	0·198	0·077
1600 largest	0·276	0·085
1776 all observed	0·331	0·094
2204 all surveyed	∞	0·134

The standard deviations of the bond lengths and angles were calculated assuming an isotropic propagation of error in the atomic positions. An inspection of the resulting correlation coefficients from least squares shows the expected correlation between the scale factor and the various isotropic temperature factors. The coefficient between the B for the iron atom and the scale factor is 0·71 while all other B factors have a coefficient with the scale factor of less than 0·2. Other coefficients of about 0·2 occur between the coordinates of bonded atoms such as a carbonyl group.

Special thanks go to the authors of various computer programs used in the analysis: Trueblood, Sparks & Gantzel for least squares; Allen Zalkin for Fourier series; A. Larson for goniostat settings.

References

Dodge, R. P. & Schomaker, V. (1960). *Nature, Lond.* **186**, 798.

Dunitz, J. D., Mez, H. C., Mills, O. S. & Shearer, H. M. M. (1962). *Helv. Chim. Acta*, **45**, 647.

Hübel, W., Braye, E. H., Clauss, A., Weiss, E., Krüerke, U., Brown, D. A., King, G. S. D. & Hoogzand, C. (1959). *J. Inorg. Nucl. Chem.* **9**, 204.